=============== **MAGNETISM** ===============

Magnetic and Electrical Properties of the Half-Metallic Ferromagnets Co_2CrAl

N. I. Kourov[a, *], A. V. Korolev[a], V. V. Marchenkov[a], A. V. Lukoyanov[a, b], and K. A. Belozerova[a]

[a] Institute of Metal Physics, Ural Branch of the Russian Academy of Sciences,
ul. Sofii Kovalevskoi 18, Yekaterinburg, 620990 Russia
* e-mail: kourov@imp.uran.ru
[b] Ural Federal University named after the First President of Russia B. N. Yeltsin
(on the basis of Ural State Technical University−UPI), ul. Mira 19, Yekaterinburg, 620002 Russia
Received October 23, 2012

Abstract—This paper presents the results of measurements of the magnetic and electrical properties of the ferromagnetic alloy Co_2CrAl in two structural states: (i) after severe plastic deformation and (ii) after short-term high-temperature annealing of the deformed specimens. The experiments have been performed at temperatures in the range from 2 to 900 K in magnetic fields $H \leq 50$ kOe. The ferromagnetic Curie temperature T_C and the paramagnetic Curie temperature Θ have been determined ($T_C = 305$ K and $\Theta = 326$ K), as well as the spontaneous magnetic moment μ_S and the effective magnetic moment μ_{eff} per molecule of the alloy ($\mu_S = 1.62$ μ_B and $\mu_{eff}^2 = 8.2$ μ_B^2). It has been shown that the magnetic crystalline anisotropy energy of the alloy is on the order of $\sim 5 \times 10^5$ erg/g. The specific features of the electrical properties are associated with the presence of an energy gap in the electronic spectrum near the Fermi level E_F and with the change in the parameters of the energy gap as a function of the temperature.

DOI: 10.1134/S1063783413050181

1. INTRODUCTION

In a number of works (see, for example, [1, 2]), it has been shown that the electronic band structure of the Heusler alloy Co_2CrAl is characteristic of half-metallic ferromagnets [3]: the subband of electrons with the spins directed along the magnetization vector (spin "up") is completely occupied, whereas the subband of electrons with the spins directed opposite to the magnetization vector (spin "down") in the vicinity of the Fermi level E_F is unoccupied. In other words, in this alloy for spin-down electrons at the Fermi level E_F, there is an energy gap, which, according to different authors [1, 2, 4, 5], has a width of 0.2−0.5 eV. The Co_2CrAl alloy in the ordered state stands out among the half-metallic ferromagnets by the ultimate spin polarization of ~100%. In this connection, the prospects for the possible use of this alloy in spintronic devices have aroused considerable interest in the study of its physical properties.

The band structure of the Co_2CrAl alloy easily transforms under the action of internal stresses, structural distortions, and, especially, effects of disorder [3, 4]. Under the influence of these factors, the band gap and the degree of spin polarization can vary over a wide range down to zero. Most likely, it is for this reason the results obtained by different authors on the magnetic and electrical properties are rather contra-

dictory. Particularly significant differences are found in the temperature dependences of the electrical resistivity $\rho(T)$. In [3, 4], the amorphization of the Co_2CrAl alloy due to ultrafast quenching of specimens at temperatures below room temperature led to a significant decrease in the electrical resistivity $\rho(T)$ and to the change in sign of the temperature resistance coefficient. This behavior of the electrical resistivity was explained by the fact that the alloy contains a mixture of metallic and semiconducting phases.

In recent years, much attention has been paid to searching for materials based on Heusler alloys with the excellent functional characteristics, including not only purposeful changes in the chemical composition of the alloys but also the use of various modern technologies for modifying their parameters. In particular, these alloys can be disordered, in addition to ultrafast quenching, under severe plastic deformation by high-pressure torsion of the specimens in Bridgman anvils. In this work, we have performed complex experimental investigations of the half-metallic ferromagnet Co_2CrAl for the purpose to reveal a correlation of the magnetic and electrical properties with the specific features of the electronic band structure and to determine their changes as a result of disordering of the specimens under severe plastic deformation by high-pressure torsion.

2. MAGNETIC PROPERTIES

Typical magnetic properties of the studied alloy after short-term high-temperature annealing of deformed specimens are demonstrated in Figs. 1–3 for a polycrystalline specimen in the form of a long rectangular prism with the calculated (according to Aharoni [6]) value of the demagnetizing factor $N = 0.148$. The measurements were performed on a Quantum Design MPMS-5XL SQUID magnetometer at the Department of Magnetic Measurements of the Institute of Metal Physics of the Ural Branch of the Russian Academy of Sciences (Yekaterinburg, Russia).

In general, the obtained experimental data are consistent with the results of the previously published investigations [4, 7]. First of all, we note the specific features of the studied alloy, which, in earlier investigations, received little attention. The magnetic hysteresis loop is characterized by the coercive force $H_C = 144$ Oe and the remanent magnetization $M_R = 32$ emu/g (see inset (a) in Fig. 1).[1] The irreversible processes of technical magnetization dominate at a magnetic field strength $H \leq |H_S| \cong 4$ kOe (inset (b) in Fig. 1).[2] These data indicate that the magnetic anisotropy energy in the studied alloy behaves noticeably. Moreover, the value of the magnetic anisotropy field H_A, apparently, should be higher than the value of H_S. More specifically, the value of H_A can be estimated as follows.

As can be seen from inset (c) in Fig. 1, the saturation magnetization, i.e., the horizontal straight line $M(H) = $ const, is not achieved up to the maximum value in our experiments $H = 50$ kOe. However, for sufficiently high values of $H > 20$ kOe, the magnetization obeys the law of approach to saturation (see inset (d) in Fig. 1) (the Akulov law [8]) for polycrystals:

$$M = M_S - 4DK^2/M_S H^2, \qquad (1)$$

where M_S is the saturation magnetization; K is the anisotropy constant; and D is the numerical factor, which is different for different types of anisotropy. Using the dependence $M(H^{-2})$ (see inset (d) in Fig. 1) and formula (1), we obtain the saturation magnetization $M_S = 45.9 \pm 0.1$ emu/g and, accordingly, the Z-projection of the magnetic moment $\mu_S = 1.62\ \mu_B$ per molecule of the Co_2CrAl alloy in the ground state ($T \cong 0$ K). For the Co_2CrAl alloy, different authors [4] note that the experimental value of μ_S lies in the range 1.5–3.0 μ_B. The calculated value of the magnetic

moment μ for the ordered state of this alloy is equal to 3 μ_B [1, 2]. One of the possible reasons for the discrepancy between theory and experiment is that all the experimental data were obtained on insufficiently structurally perfect specimens. In particular, the experiments were carried out using polycrystalline specimens prepared, as a rule, by arc melting, which can lead to a nonuniform distribution of the components in the specimen, to the impossibility of reaching a high degree of atomic order, and, consequently, to some differences between the real band structure and the calculated band structure.

The Co_2CrAl alloy has a cubic structure of the $L2_1$ type; therefore, the magnetic crystalline anisotropy in this alloy should also be cubic. In this case, we have $D = 2/105$, which, in turn, allows us to find, from the experiment (see inset (d) in Fig. 1), the magnetic anisotropy constant $K = 4.6 \times 10^5$ erg/g and the magnetic anisotropy field $H_A = 2K/M_S = 20$ kOe. The errors in the determination of these quantities do not exceed a few percent. The estimates of the magnetic anisotropy parameters are considered only as a first approximation, and, further, we will make some refinements of the magnetic anisotropy of the specimen.

According to the well-known theoretical descriptions of the isotherm $M(H)$, the relative remanent magnetization $m_R = M_R/M_S$ for a polycrystalline specimen depends on the number of equivalent crystallographic axes of easy magnetization (EMA). In the case of cubic anisotropy, the characteristic orientations of the easy magnetization axes, as a rule, are crystallographic directions either of the $\langle 100 \rangle$ type (three equivalent easy magnetization axes, $K_3 > 0$, K_n is the cubic anisotropy constant, and n is the number of equivalent easy magnetization axes) or of the $\langle 111 \rangle$ type ($K_4 < 0$). With an increase in the number of equivalent directions of the easy magnetization axes, the relative remanent magnetization m_R increases and amounts to 0.83 ($K_3 > 0$) and 0.87 ($K_4 < 0$).

For the studied specimen in the ground state ($T \cong 0$ K), we have the experimental value of $m_R^{exp} = 0.70$, which is significantly less than the minimum possible theoretical value of m_R for the cubic type of magnetic crystalline anisotropy and is substantially higher for the case of uniaxial anisotropy with a single preferred easy magnetization axis ($K_1 > 0$, $m_R = 0.5$). This circumstance ($0.50 < m_R^{exp} < 0.83$) suggests that the magnetic anisotropy in the studied specimen has a more complex type as compared to the simple case of cubic or uniaxial anisotropy. One of the possible explanations for the quantitative disagreement between the experimental value m_R^{exp} and theoretical estimates can be given in the framework of the combined Stoner–Wohlfarth model for the case of the uniaxial anisotropy superimposed on the cubic anisotropy [9]. Such

---

[1] The remanent magnetization M_R was determined taking into account the demagnetizing factor of the specimen, i.e., at the point in which the demagnetization curve intersects the straight line $M = H/Nd$, where $d = 8.04$ g/cm^3 is the density of the material.

[2] Here, H_S is the critical field at which the ascending and descending branches of the hysteresis loop merge into a single line.
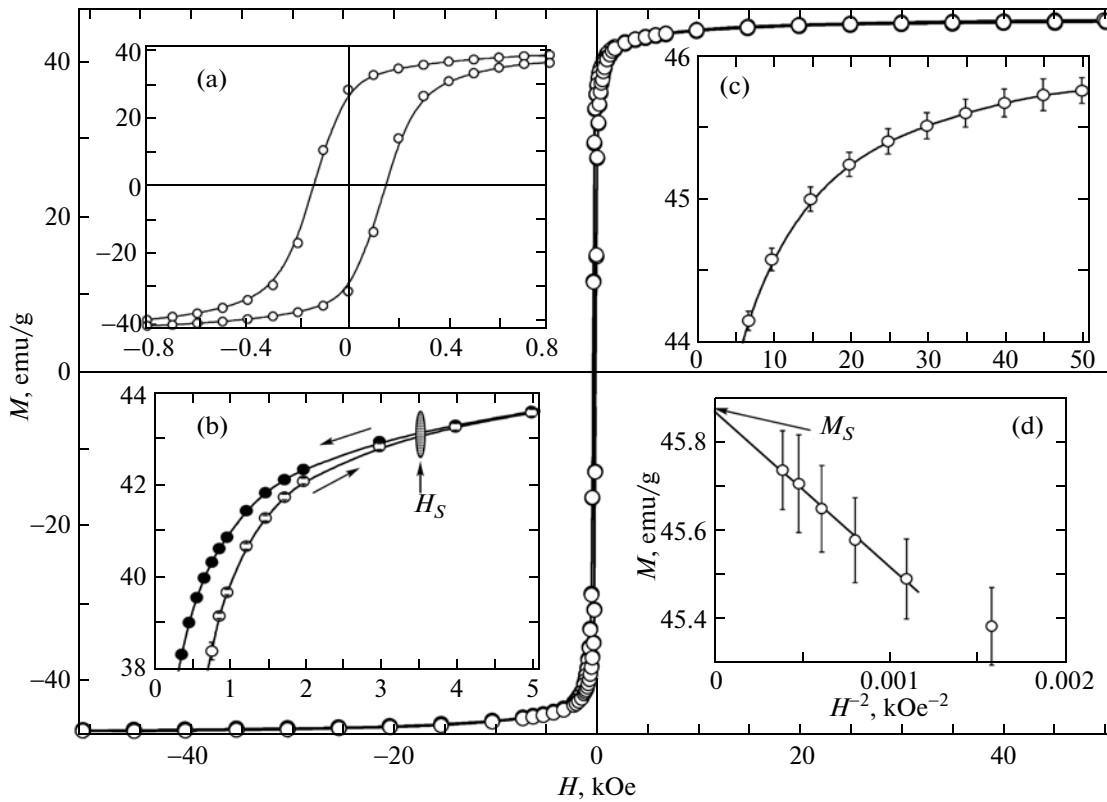
Fig. 1. Magnetization of the Co_2CrAl alloy at a temperature $T = 2$ K. Insets (a)−(c) show the magnetization curves in weak and strong magnetic fields. Inset (d) shows the dependence $M(H^{-2})$.

a mixed anisotropic state is expected and was previously experimentally investigated in a number of works [9−11].

As was noted in [4, 5], one of the characteristic features of the studied alloy is associated with tetragonal distortions of the structure due to the incomplete atomic ordering. It is reasonable to assume that this type of structural distortions can be responsible for the uniaxial anisotropy induced as a supplement to the cubic anisotropy. Based on this assumption, we analyze the data presented in Fig. 1 in the framework of the model described in [9] and determine the parameters of the combined anisotropy: $H_{A1} = 2K_1/M_S$, $H_{A3} = 2K_3/M_S$, and $H_{A4} = 2K_4/M_S$, where H_{A1} and H_{A3}, H_{A4} are the uniaxial and cubic anisotropy fields for $K_3 > 0$ and $K_4 < 0$, respectively. In order to solve this problem, we should find the coefficient D_{kU} in the equation

$$M/M_S = 1 - D_{kU}/H^2 \qquad (2)$$

by appropriately reconstructing the plot in inset (d) to Fig 1. The value of this coefficient is determined as

$$D_{kU} = H_{A1}^2/15 + H_{An}^2/105. \qquad (3)$$

We should also determine one more parameter, i.e., $k_U(m_R)$, which is a function of the magnetization m_R and characterizes the relative contribution of the

uniaxial anisotropy to the total magnetic anisotropy energy. In the analytical form, the function $k_U(m_R)$ has yet not been obtained; therefore, it has been found numerically. The plots of this function are given in [9]. Using these plots, it is easy to find numerical values of $k_U(m_R)$, which, in turn, are determined as

$$k_U(m_R) = H_{A1}/(H_{A1} + H_{An}). \qquad (4)$$

In our experiment, we have $m_R^{exp} = 0.7$; the value of $k_U(m_R)$ is equal to 0.336 or 0.221 for $K_3 > 0$ or $K_4 < 0$, respectively; and the coefficient is $D_{kU} = 7.7 \times 10^6$ Oe^2. Next, we solve equations (3) and (4) and find the desired anisotropy parameters, for which the numerical values with an error of no more than 5% are presented in the table.

The performed analysis has demonstrated that the cubic magnetic anisotropy energy in the Co_2CrAl alloy, regardless of the method used for its determination, is very high and comparable to that for some alloys of 3d metals. The use of the model proposed in [9] provides additional information about the specificity of the magnetic anisotropy of the studied specimen and its possible characteristics. However, the obtained results leave a number of questions about the magnetic anisotropy of the Co_2CrAl alloy open. First of all, it is a question about the sign of the anisotropy constant
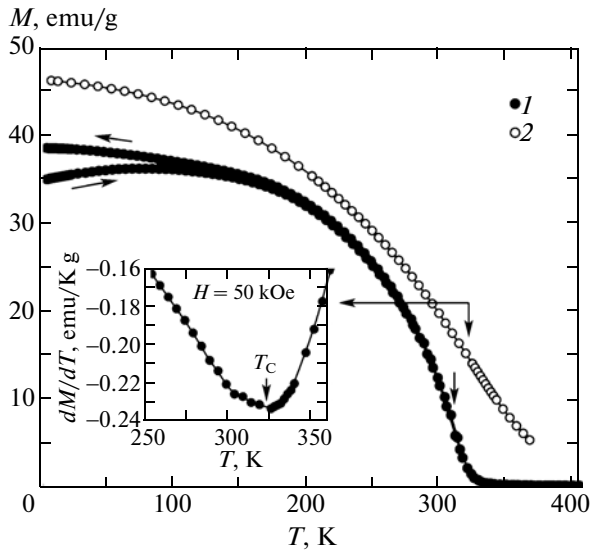
Fig. 2. Temperature dependences of the magnetization in magnetic fields $H = $ (*1*) 0.5 and (*2*) 50 kOe. Arrows along the curves indicate the direction of the temperature change. The inset shows the dependence $dM/dT(T)$ determined for the case of $H = 0.5$ kOe.
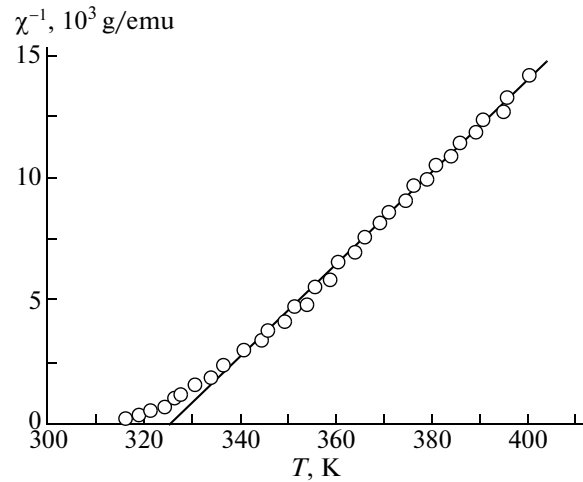

Fig. 3. Paramagnetic susceptibility of the Co_2CrAl alloy. The solid line represents the result of the data processing in accordance with expression (5).

K_n, as well as the questions about the physics underlying both the basic cubic anisotropy and the additional uniaxial anisotropy in the studied alloy and other semi-metallic ferromagnetic alloys. The solution of these problems, probably, is possible in the study of single crystals and with the further development of the physics of magnetism of Heusler alloys. At present, we do not have single-crystal specimens and cannot give more detailed information on the magnetic anisotropy of the Co_2CrAl alloy. We note only that the possibility of obtaining a high magnetic anisotropy energy in alloys based on Co_2CrAl was predicted in [12], where the high values of orbital atomic magnetic moments of the Cr and Co ions were found experimentally. It is also relevant to note that the results presented in [12] and the confirmation which we obtained for the prediction made in that work suggest a high level of anisotropic linear magnetostriction in alloys based on Co_2CrAl.

The temperature dependence of the magnetization presented in Fig. 2 was measured according to the fol-

Magnetic anisotropy parameters at $T = 2$ K determined from the experimental data (see inset (d) in Fig. 1) in the framework of the combined Stoner–Wohlfarth model for the case of superposition of the uniaxial anisotropy on the cubic anisotropy [9]

n	H_{A1}, kOe	H_{An}, kOe	K_1, 10^5 erg/g	K_n, 10^5 erg/g
3 ($K_3 > 0$)	8.6	17.0	2.0	3.9
4 ($K_4 < 0$)	6.5	22.7	1.5	−5.2

lowing scheme: the specimen at $H = 0$ is cooled to the temperature $T = 2$ K, then the magnetic field $H = 0.5$ kOe $\ll H_S$ is turned on, and the functions $M(T)$ are measured in the specified field in the cycle of continuous heating of the specimen to the paramagnetic state, followed by cooling to $T = 2$ K. It can be seen that the obtained dependence $M(T)$ is characterized by the effect of temperature hysteresis. In [4, 13], this feature in the behavior of the dependence $M(T)$ was attributed to the possible existence of atomically ordered and disordered regions in the alloy, which can be accompanied by the emergence of competing ferromagnetic and antiferromagnetic interactions. In this case, we should expect the effect of unidirectional magnetic anisotropy. However, in our specimens, this effect has not been found. In our view, the temperature hysteresis of the dependence $M(T)$, which was measured at a sufficiently low magnetic field strength $H \ll H_S(T = 2$ K$) \cong 4$ kOe, is a typical consequence of temperature changes in the magnetic hysteresis loop for ferromagnetic specimens, namely, a decrease in the coercive force H_C and the critical field H_S with increasing temperature, i.e., a consequence of the specifics of the irreversible technical magnetization processes, primarily the processes of irreversible displacement of domain walls under the action of the resulting internal magnetic field, which, for a uniform magnetization of the specimen, can be defined as $H_i(T) = H - NM(T)d$ (where N is the demagnetizing factor of the specimen and $d = 8.04$ g/cm^3 is the density of the material).

The fact that the temperature hysteresis of the polytherm $M(T)$ is actually a consequence of the temperature changes in the isotherm $M(H)$ is confirmed as follows. From a comparison of the data presented in Figs. 1 and 2, we can seen that, upon heating, the starting point ($T = 2$ K, $H = 0.5$ kOe), which should lie on the initial magnetization curve passing inside of the

hysteresis loop, is located directly on the ascending branch of the hysteresis loop, while the end point of the temperature cycle is located on the descending branch. We assume that the magnetic hysteresis loop over a wide temperature is determined by the irreversible effects of rearrangement of the magnetic domain structure due to changes in the internal magnetic field $H_i(T)$. In other words, during the measurement $M(T)$, the external magnetic field H remains unchanged, whereas the internal magnetic field H_i changes with variations in the magnetization M. It is under the action of this resulting field H_i in a certain temperature range, there occur irreversible processes of transformation of the domain structure and, consequently, the processes of magnetization of the specimen during heating and its demagnetization during cooling.

As can be seen from Fig. 2, the dependence $M(T)$ at $H = 50$ kOe $> H_A \gg H_S$ is a single-valued function; i.e., the temperature changes in the magnetization during heating and cooling in this case have a reversible character.

The experimental data presented in Fig. 2 allow us to determine the Curie temperature T_C as the position of the inflection point on the curves $M(T)$, which can be found as the minimum in the dependence dM/dT (see inset in Fig. 2). For the experiment with $H = 0.5$ and 50.0 kOe, the Curie temperatures T_C obtained by this means with an accuracy of $\sim 1-2$ K are equal to 308 and 318 K, respectively. A detailed discussion of the method used to determine the values of the Curie temperature T_C is beyond the scope of the present paper. At the same time, from general considerations it follows that, with an increase in the magnetic field strength H, the inflection point of the function $M(T)$ should shift toward higher temperatures, and the result obtained at a lower value of H is more reliable; i.e., the value of $T_C = 308$ K can be taken as the true value of the Curie temperature of the studied alloys.

The results of measurements of the magnetic susceptibility at temperatures above T_C are presented in Fig. 3. It can be seen that, over a wide temperature range, the magnetic susceptibility within the measurement error is described by the Curie–Weiss law

$$\chi = C/(T - \Theta). \tag{5}$$

Here, C is the Curie constant; Θ is the Weiss constant (or the paramagnetic Curie temperature); the numerical values of these constants are 0.0052 K cm³/g and 326 K, respectively; and the square of the effective magnetic moment μ_{eff}^2 per formula unit is equal to 8.2 μ_B^2. Using the data obtained from the low-temperature measurements presented in Fig. 1, we find the spontaneous magnetic moment μ_S per formula unit at saturation ($\mu_S = 1.62 \mu_B$) and determine the Rhodes–Wohlfarth parameter $p_{\text{R-W}} = p_C/\mu_S = 1.26$, where the quantity p_C is found from the solution of the equation

$p_C(p_C + 2) = \mu_{\text{eff}}^2$ [14]. The obtained value of $p_{\text{R-W}}$ is typical of $3d$ metals, which indicates an insufficiently complete localization of magnetic moments on individual atoms.

3. CALCULATIONS OF THE ELECTRONIC STRUCTURE

In order to refine the structural features of the electronic spectrum of the considered alloy, we performed the band structure calculations using the tight-binding linear muffin-tin orbital method in the atomic sphere approximation (Stuttgart TB-LMTO-ASA program, version 47) [15]. The orbital basis set included orbitals corresponding to the $4s$, $4p$, and $3d$ states of the Co and Cr ions, as well as to the $3s$, $3p$, and $3d$ states of the Al ions. We used a grid of 47 irreducible k-points in the first Brillouin zone (the total number of k-points was 1000). The obtained energy dependences of the electron densities of states (d, s, p) for the case of ferromagnetic (the spin-polarized calculation in the local spin density approximation (LSDA)) and nonmagnetic (the calculation in the local density approximation (LDA) without spin polarization) states of the Co₂CrAl alloy are shown in Fig. 4.

It should be noted that the results of the spin-polarized calculation, in general, coincide with those published earlier (see, for example, [1, 2]). It can be seen from the figure that, near the Fermi level E_F for electrons with the spins directed along the magnetization vector, there is a band of electron densities of states with a width of approximately 1 eV and with several narrow peaks, which is formed predominantly by the d states. By contrast, for electrons with the spins directed opposite to the magnetization vector in the vicinity of the Fermi level E_F, there is a deep energy gap also with a width of approximately 1 eV. According to the band structure calculations, the magnetic moments on individual atoms are as follows: for cobalt atoms $\mu_{\text{Co}} = 0.75 \mu_B$, for chromium atoms $\mu_{\text{Cr}} = 1.56 \mu_B$, and for aluminum atoms $\mu_{\text{Al}} = -0.06 \mu_B$. The total magnetic moment per formula unit (f.u.) is equal to 3 μ_B, which is significantly higher than the experimental values of the spontaneous magnetic moment μ_S, but almost completely coincides with the value of the effective magnetic moment μ_{eff}. Accordingly, the calculated densities of states at the Fermi level are as follows: for the d electrons $n_F(d) = 4.52$ states/eV f.u., for the s-electrons $n_F(s) = 0.06$ states/eV f.u., and for p-electrons $n_F(p) = 0.15$ states/eV f.u. The total density of states at the Fermi level E_F in the ferromagnetic state is equal to $n_F(E_F) = 4.73$ states/eV f.u. This value of the electron density of states is slightly higher than that obtained in [2].

In the disordered state (the LDA calculations), the structure of the electronic spectrum, especially near the Fermi level E_F, undergoes significant changes. In
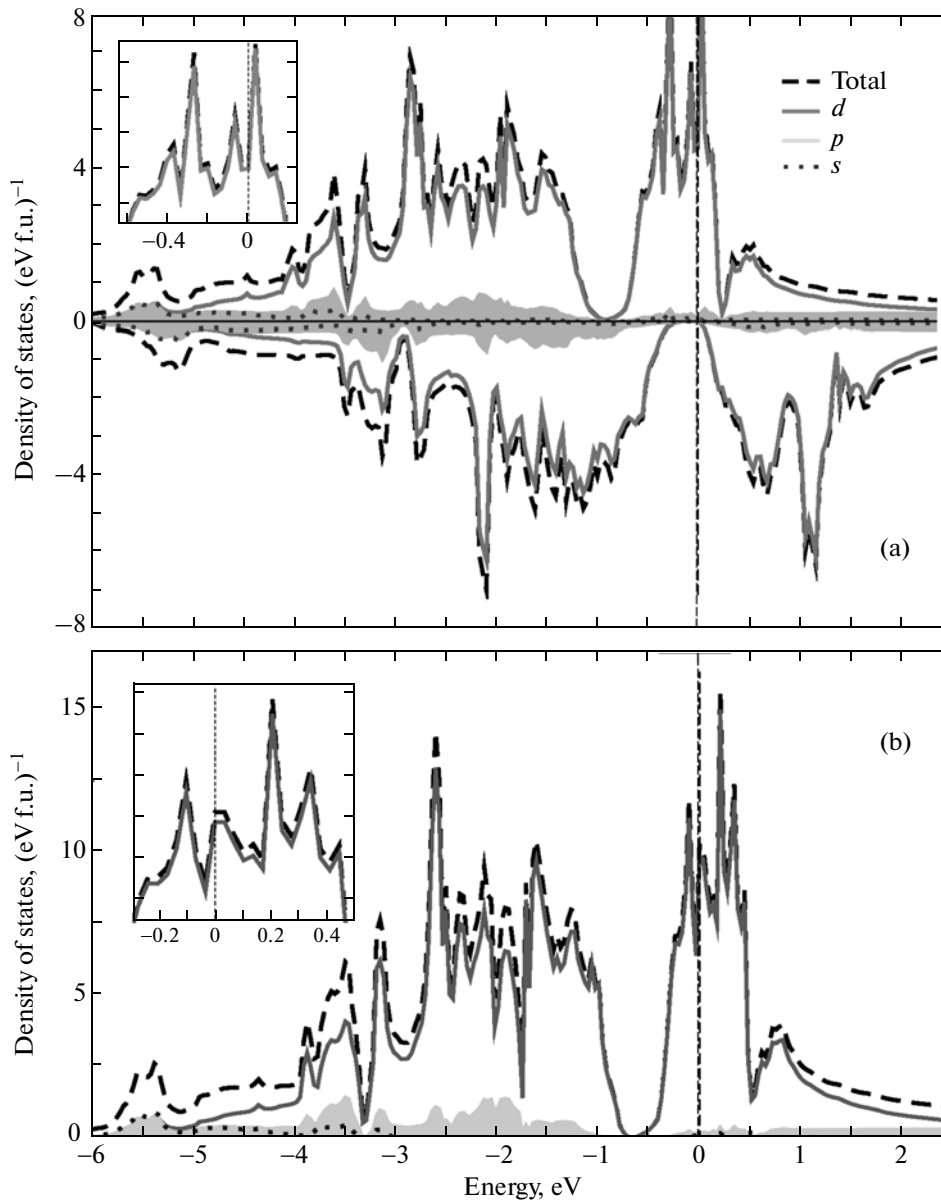
Fig. 4. Calculated densities of states for the Co_2CrAl alloy in the (a) ferromagnetically ordered state (the spin-polarized LSDA-calculation) and (b) disordered state (the LDA calculation without spin polarization). The insets show the densities of states near the Fermi level E_F.

the vicinity of the Fermi level E_F, there is a band of electron densities of states, which is formed predominantly by the d electrons with different spin directions. Accordingly, the magnetic moment in the disordered state is zero, and the electron densities of states at the Fermi level E_F take the following values: for the d electrons $n_F(d) = 9.84$ states/eV f.u., for the s electrons $n_F(s) = 0.16$ states/eV f.u., and for the p-electrons $n_F(p) = 0.31$ states/eV f.u. The total densities of states at the Fermi level E_F in the disordered state is equal to $n_F(E_F) = 10.31$ states/eV f.u. Consequently, because of the "collapse" of the energy gap in the electronic spec-

trum, the total density of states at the Fermi level E_F increases by a factor of more than 2.

4. ELECTRICAL PROPERTIES

The specific features in the behavior of electrical properties of the half-metallic ferromagnet Co_2CrAl are illustrated by the results of measurements of the temperature dependences of the electrical resistivity $\rho(T)$ and the absolute differential thermoelectric power $S(T)$ presented in Figs. 5–7. Taking into account the rather unusual effect of increase in the electrical resistivity $\rho(T)$ after annealing of the
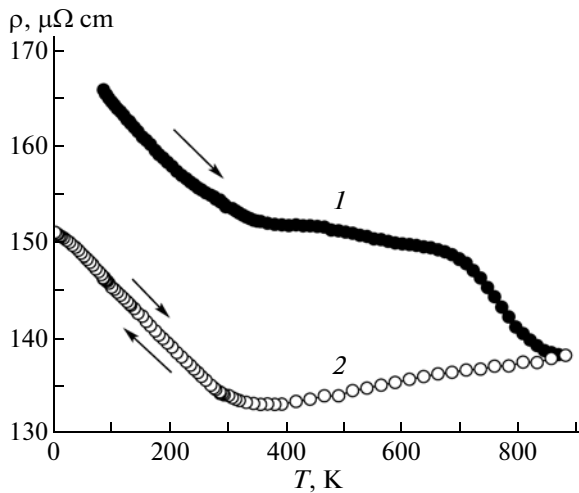
Fig. 5. Temperature dependences of the electrical resistivity $\rho(T)$ measured for (*1*) the plastically deformed (disordered) Co_2CrAl alloy and (*2*) the Co_2CrAl alloy annealed at $T \sim 900$ K. Arrows indicate the direction of the temperature change.

Fig. 6. Electrical resistivity of the atomically ordered Co_2CrAl alloy at a temperature $T \ll T_C$ as a function of the square of the magnetization measured at $H = 50$ kOe.

Co_2CrAl amorphous alloy, which was revealed in [4, 5], we performed the disordering of the studied specimens under severe plastic deformation by torsion in Bridgman anvils turned through five revolutions at a high pressure $P = 10$ GPa. As a result of this disordering of the specimens, there occurred a transition from the coarse-grained state (with a grain size of 100−500 μm) to the nanocrystalline state (with a grain size of 10−20 nm) [16]. In contrast to [4, 5], in our case, we observed an increase in the electrical resistivity due to the disordering of the alloy at room temperature by ~14%. As can be seen from Fig. 5, the subsequent heating leads to an irreversible decrease in the electrical resistivity $\rho(T)$ in the temperature range 700−900 K down to values typical of the atomically ordered Co_2CrAl alloy. Further, the behavior of the dependence $\rho(T)$ becomes reversible.

The electrical resistivity of the studied alloy has two key features: (i) an unusually high value of the electrical resistivity of the metallic specimen at $T \sim 0$ K ($\rho_0 > 130$ μΩ cm) and (ii) the revealed change in sign of the temperature resistance coefficient with a change in the magnetic state near the Curie temperature T_C. The causes for the high value of the electrical resistivity and the negative temperature resistance coefficient in the magnetically ordered state of the Co_2CrAl alloy were discussed in several papers. A detailed analysis of these works is given in [5]. As a rule, the observed features in the behavior of the dependence $\rho(T)$ are explained by the existence of the spin or structural disorder in the studied alloys, which leads to the localization of conduction electrons. The electrical properties in these works are usually considered in terms of the charge carrier hopping mechanism. It is known (see, for example, [17]) that, in the case of hopping conduc-
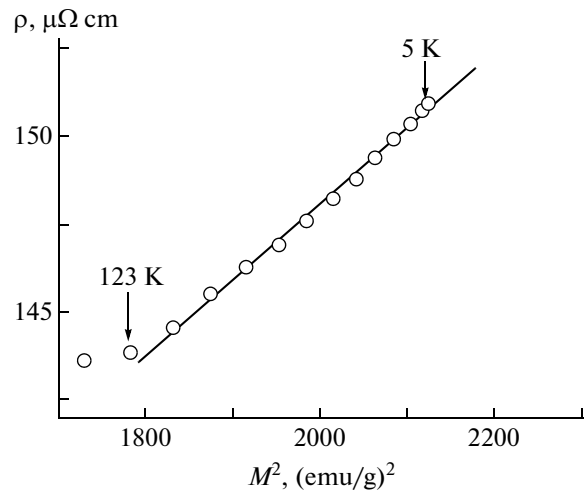
tion, the temperature dependence of the electrical conductivity $\sigma = \rho^{-1}$ should have an exponential form. However, the processing of our data on the measurements of the dependence $\sigma(T)$ according to the exponential law did not give satisfactory results in a reasonable range of temperatures, which casts doubt on the explanation of the specific features in the behavior of the electrical properties of the Co_2CrAl alloy only in terms of the hopping conduction mechanism.

For magnetically ordered alloys of the considered type, which have an energy gap in the electronic spectrum, the electrical resistivity and its temperature dependence should be determined, primarily, by the parameters of the spectrum near the Fermi level E_F. In
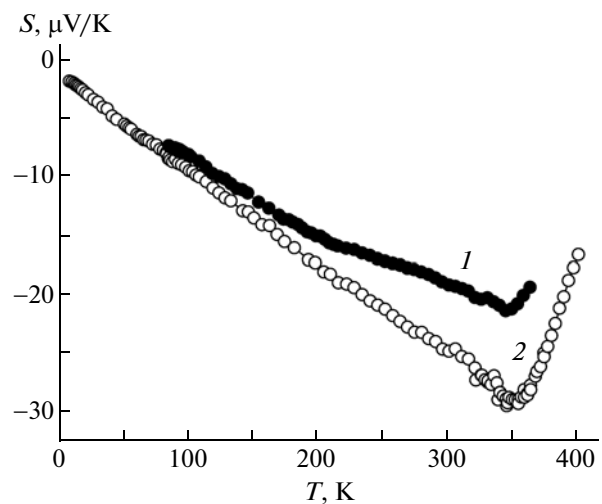

Fig. 7. Temperature dependences of the thermoelectric power $S(T)$ measured for (*1*) the plastically deformed (disordered) Co_2CrAl alloy and (*2*) the Co_2CrAl alloy annealed at $T \sim 900$ K.

turn, the parameters of the electronic spectrum depend on the spontaneous magnetization. According to [18, 19], in the simplest case, when the change in the magnetic state is insignificant, for the magnetic component of the electrical resistivity $\rho_m(T)$ we have the expansion in the magnetization:

$$\rho(T) = \rho(0) + aM_S^2, \qquad (6)$$

where $\rho(0)$ includes the temperature-independent residual resistivity, the temperature-dependent electron–electron component ρ_{ee}, and the temperature-dependent electron–phonon component ρ_{ph}; a is a coefficient, which, in our case, has a positive sign. In order to verify this hypothesis, we consider the dependence $\rho(T) \sim M^2$ ($H = 50$ kOe) shown in Fig. 6. It can be seen that, for the atomically ordered Co_2CrAl alloy, relationship (6) is satisfied over a relatively wide temperature range at $T \ll T_C$, where $M_S \sim M$ ($H = 50$ kOe) due to the weakly pronounced para-process. Of course, in this case, the components ρ_{ee} and ρ_{ph} at low temperatures are assumed to be relatively small.

The violation of relationship (6) at higher temperatures is primarily associated with the enhancement of the para-process, when the value of M_S significantly deviates from M ($H = 50$ kOe), as well as with the substantial increase in the component ρ_{ph}. In addition, at temperatures $T \longrightarrow T_C$, there are strong changes in the parameters of the electronic spectrum near the Fermi level E_F, which should lead to significant changes in the kinetic properties and the violation of relationship (6). This situation was considered in [18, 19] for antiferromagnetic metals, which have an energy gap in the electronic spectrum at the Fermi level E_F.

In the atomically ordered Co_2CrAl alloy, the transition to the paramagnetic state due to the vanishing of the spontaneous magnetization leads to the disappearance of the "separation" between the subbands with different spin directions, as can be seen from our band structure calculations in the local electron density approximation (LDA) without spin polarization (Fig. 4b). Accordingly, the magnetic component of the electrical resistivity at temperatures $T > T_C$ reaches saturation and, with a further increase in the temperature, remains constant. Despite the sufficiently high values of the electrical resistivity, the dependence $\rho(T)$ at temperatures above T_C acquires a normal shape for metals with the positive temperature resistance coefficient due to the electron–phonon scattering of conduction electrons at $T > \theta_D$ (here, θ_D is the Debye temperature).

As is known [20], the thermoelectric power of metallic ferromagnets is determined by the "separation" of the subbands with mutually opposite spin directions,

$$S = -(\pi^2 k_B^2 T/3e)\left[\frac{3}{2}E_F - \frac{n_d'(\uparrow) + n_d'(\downarrow)}{n_d(\uparrow) + n_d(\downarrow)}\right]_{E_F}. \qquad (7)$$

In expression (7), arrows indicate the densities of states n_d and their first derivatives n_d' at the Fermi level E_F for the d subbands of electrons with the spins directed along the magnetization vector ($\uparrow$) and the spins directed opposite to the magnetization vector ($\downarrow$). According to our band calculations and those performed in [1, 2], for the Co_2CrAl alloy in the ferromagnetic state (in the case of the spin-polarized calculation), there are no spin-down d electrons at the Fermi level E_F; i.e., the thermoelectric power is predominantly determined by the parameters of the d subband with spin-up electrons. For this subband in the vicinity of the Fermi level E_F, the electronic spectrum has a multi-peak structure. The calculation of the electronic structure without regard for the polarization of electrons has demonstrated that the Fermi level in the Co_2CrAl alloy is also located in a broad band with several narrow peaks. Therefore, the electron density of states at the Fermi level will vary depending on the temperature smearing, which was not used in these calculations, and on the electron–electron interaction considered in the presented calculations in the framework of the local electron (spin) density approximation. All these factors complicate an unambiguous determination of the sign of the derivative $n_d'(\uparrow)$ and, consequently, a comparison of the signs of the thermoelectric power, which follow from the band calculations and from the experiments.

The experimentally revealed change in the sign of the slope of the dependence $S(T)$ upon the transition to the paramagnetic state is naturally explained by the change in the main mechanism of scattering of conduction electrons [20]. In the magnetically ordered state, the electrical properties of the considered alloys are determined primarily by the parameters of the energy gap in the electronic spectrum and, at temperatures $T > T_C$, by the mechanism of electron–phonon scattering of conduction electrons.

5. CONCLUSIONS

Thus, the investigations performed in this work have demonstrated that the disordering of the alloy under severe plastic deformation by torsion in Bridgman anvils turned through five revolutions under a pressure $P = 10$ GPa does not lead to significant changes in the electrical and magnetic properties of the material. It has been found that this alloy has a high magnetic anisotropy energy ($\sim 5 \times 10^5$ erg/g). The behavior of the electrical properties (electrical resistance and thermoelectric power) can be associated with the presence of an energy gap in the electronic spectrum near the Fermi level E_F, and their values and temperature dependences are satisfactorily explained by taking into account the changes in the parameters of the electronic spectrum at the Fermi level as a function of the spontaneous magnetization.

REFERENCES

1. T. Block, M. J. Garey, B. A. Gurney, and O. Jepsen, Phys. Rev. B: Condens. Matter **70**, 205114 (2004).

2. M. Zhang, Z. Liu, H. Hu, G. Liu, Y. Cui, J. Chen, G. Wu, X. Zhang, and G. Xiao, J. Magn. Magn. Mater. **277**, 130 (2004).

3. V. Yu. Irkhin and M. I. Katsnel'son, Phys.—Usp. **37** (7), 659 (1994).

4. Y. V. Kudryavtsev, V. N. Uvarov, V. A. Oksenenko, Y. P. Lee, J. B. Kim, Y. H. Hyun, K. W. Kim, J. Y. Rhee, and J. Dubowik, Phys. Rev. B: Condens. Matter **77**, 195104 (2008).

5. Y. V. Kudryavtsev, Y. P. Lee, Y. J. Yoo, M. S. Seo, J. B. Kim, Y. S. Hwang, J. Dubowik, K. W. Kim, E. H. Choi, and O. Prokhnenko, Eur. Phys. J. B **85**, 19 (2012).

6. A. Aharoni, J. Appl. Phys. **83**, 3432 (1998).

7. M. Hakimi, P. Kameli, and H. Salamati, J. Magn. Magn. Mater. **322**, 3443 (2010).

8. N. S. Akulov, *Ferromagnetism* (GONTI, Moscow, 1939) [in Russian].

9. V. A. Ignatchenko, R. S. Iskhakov, and G. V. Popov, Sov. Phys. JETP **55** (5), 879 (1982); http://www.kirensky.ru/zdoc/ssi.pdf.

10. A. V. Korolyov, V. S. Gaviko, and N. V. Mushnikov, Phys. Status Solidi A **119**, K163 (1990).

11. N. V. Mushnikov, A. V. Korolyov, V. S. Gaviko, Ye. I. Raevski, and L. Pareti, J. Appl. Phys. **70**, 2768 (1991).

12. H. J. Elmers, G. H. Fecher, D. Valdaitsev, S. A. Nepijko, A. Gloskovskii, G. Jakob, G. Schonhense, S. Wurmehl, T. Block, C. Felser, P.-C. Hsu, W. L. Tsai, and S. Gramm, Phys. Rev. B: Condens. Matter **67**, 104412 (2003).

13. J. Dubowik, I. Goscianska, Y. V. Kudryavtsev, and V. A. Oksenenko, Mater. Sci. Pol. **25**, 1281 (2007).

14. P. Rhodes and E. P. Wohlfarth, Proc. R. Soc. London, Ser. A **273**, 247 (1963).

15. O. K. Andersen, Z. Pawlowska, and O. Jepsen, Phys. Rev. B: Condens. Matter **34**, 5253 (1986).

16. V. V. Marchenkov, L. A. Fomina, E. P. Platonov, N. I. Kourov, E. B. Marchenkova, V. G. Pushin, E. I. Shreder, N. A. Viglin, T. P. Tolmachev, V. P. Pilyugin, A. V. Korolev, and Kh. V. Veber, in *Abstracts of Papers of the 36th Workshop on Low-Temperature Physics, St. Petersburg, Russia, July 2–6, 2012* (St. Petersburg, 2012), p. 215.

17. N. Mott and E. Davis, *Electronic Processes in Non-Crystalline Materials* (Oxford University Press, Oxford, 1971; Mir, Moscow, 1974).

18. V. Yu. Irkhin and Yu. P. Irkhin, *Electronic Structure, Correlation Effects, and Physical Properties of d- and f-Metals and Their Compounds* (Ural Branch of the Russian Academy of Sciences, Yekaterinburg, 2004; Cambridge International Science, Cambridge, 2007).

19. Yu. P. Irkhin, Fiz. Met. Metalloved. **4**, 214 (1958).

20. F. J. Blatt, P. A. Schroeder, C. L. Foiles, and D. Greig, *Thermoelectric Power of Metals* (Plenum, New York, 1976; Metallurgiya, Moscow, 1980).

Translated by O. Borovik-Romanova